Study the grain boundary triple junction segregation of phosphorus in a nickel-base alloy using energy dispersive X-ray spectroscopy on a transmission electron microscope

Tian, Jinsen; Chiu, Yu Lung

DOI:
10.1016/j.matchar.2018.12.021

License:
Other (please provide link to licence statement

Document Version
Peer reviewed version

Citation for published version (Harvard):
Tian, J & Chiu, YL 2019, 'Study the grain boundary triple junction segregation of phosphorus in a nickel-base alloy using energy dispersive X-ray spectroscopy on a transmission electron microscope', *Materials Characterization*, vol. 148, pp. 156-161. https://doi.org/10.1016/j.matchar.2018.12.021

Study the grain boundary triple junction segregation of phosphorus in a nickel-base alloy using energy dispersive X-ray spectroscopy on a transmission electron microscope

Abstract

Segregation of phosphorus at grain boundary triple junctions in a nickel-base alloy was measured using energy dispersive X-ray spectroscopy on a transmission electron microscope. It was found that the triple junction segregation of phosphorus varies with grain boundaries in that the concentration of phosphorus at triple junction can be higher or lower than that at the adjacent grain boundaries. A concentration gradient was detected along some grain boundaries within a distance of 5-100 nm from the associated triple junctions. The results are discussed with regards to various structural and atomistic diffusion characteristics.

Keywords: Triple junction segregation; Energy dispersive X-ray spectroscopy (EDS); Transmission electron microscope; Ni-base alloy.

1. Introduction

Phosphorous (P) has traditionally been regarded detrimental in nickel (Ni)-base superalloys as it segregates to the grain boundary (GB) and reduces the GB cohesion [1, 2]. However, some evidences have also been found that P can be beneficial for the stress rupture life of wrought superalloys also due to its GB segregation [3-5]. Some research has been done on the GB Segregation of P in Ni-base alloys [6, 7]. Compared with GB segregation, segregation of P to GB triple junctions (TJs) has rarely been reported [8]. TJs, as line defects in their own right with specific kinetic and thermodynamic properties, have received some attentions recently [9, 10]. They can act as fast diffusion path due to the larger free volume compared with grain boundary, which has been confirmed by diffusion experiments and molecular dynamics modelling [10-14]. Nucleation can start from the TJ during recrystallization as it has much larger misorientaion gradient compared with GBs [15]. TJ can also serve as the

nucleation site during phase transformation because of the removal of interfacial material by forming an embryonic secondary phase [9]. With a low mobility, it can exert a drag effect on the GB motion and slow down the grain growth [16]. Also, TJ affects the mechanical properties. For example, they have been identified as the crack nucleation site during high temperature creep where GB sliding happened [17]. Albeit the above studies on the TJ structure, diffusion and mobility, the study on the TJ chemical segregation has been very limited [18-22] and the possible reasons for this could be 1) geometrically a GB TJ could assume very different 3D configurations depending on the constituent grain boundaries such that the TJ could be very complex particularly when the grain sizes are very small. 2) Even when the grain sizes are large and that the TJs can be simplified as a line defect, the TJs need to be aligned with the electron beam direction before any meaningful high resolution microanalysis (for example using energy dispersive X-ray spectroscopy (EDS)) can be achieved, which is experimentally difficult and not always possible for instance due to the specimen geometry. Traditionally the EDS detector on a TEM is located to one side of the microscope such that the specimen needs to be tilted to a specific angle to maximise the X-ray signals detectable which makes the alignment of the TJ with the electron beam even more challenging [19]. Due to the complex TJ structure, even computer simulations were only performed on those junctions associated with special GBs, such as Σ3 twin boundaries [23]. In this work, an advanced TEM associated with the Chemi-STEM^{TM} technology which consists of four symmetrically positioned EDS detectors was used to measure the segregation of phosphorus at TJs associated with random high angle GBs in a nickel-base alloy.

2. Materials and Methods

The alloy was prepared by arc melting of Ni, Al and Ni_2P with a purity of 99.99%, 99.995% and 99.95% respectively according to the nominal alloy composition of Ni-6%Al-0.1%P

(at %). The alloy button was re-melted twice in order to reduce the porosity and improve the chemical homogeneity. The alloy was homogenized in a quartz tube filled with argon at 1300 ºC for 48 hours. The grain size of the as-homogenised samples is more than 1 mm. In order to reduce the grain size of the as-homogenised samples so that making the observing grain boundary triple junctions in the standard TEM discs, the homogenized alloy was then compressed by 60% and then annealed at 700 ºC for 2 hours followed by water quenching. TEM foils were prepared by twin-jet polishing using a solution containing 5% $HClO_4$ and 95% C_2H_5OH, at a current of 0.05 A and a temperature of -25 ºC and characterized using an FEI Talos F200 microscope operated at 200 kV. The Super-X detection system on the Talos F200 consists of four windowless silicon drifted detectors each of 30 mm^2 active area offering the maximum solid angle of 0.9 srad and the X-ray collection efficiency maintains high between -25 degrees and +25 degrees of tilting [24]. For the current study, the electron probe size of 0.73 nm was used.

3. Results

Fig. 1(a) shows the EBSD orientation image map obtained from the quenched sample. The averaged grain size is about 40µm. Most of the TJs are composed of random GBs rather than Σ3 twin boundaries. An SEM image obtained from the sample used for TEM EDS measurement is shown in Fig.1b.

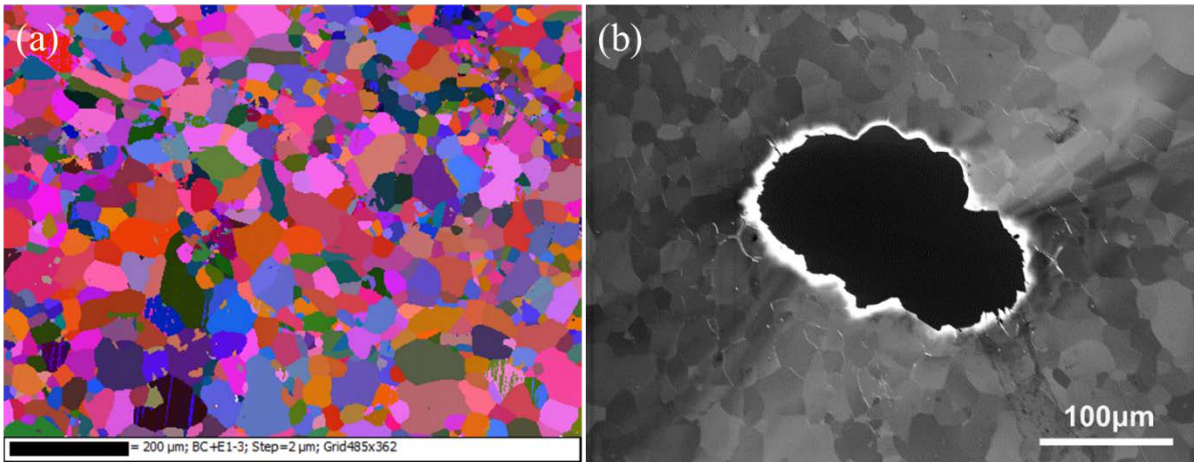

Fig.1 (a) EBSD orientation map and (b) secondary electron image of the sample

Figs. 2(a&b) show the high angle annual dark field (HAADF) images of two TJs (named TJ-I and TJ-II) where in each case all 3 constituent GBs were tilted to be aligned with the electron beam. The misorientation angles and axes associated with individual GBs were determined and listed in Table 1. The P concentration measured from interior of different grains remains the same of 0.1 at%. The EDS Spectra collected from the TJs (shown in a & b) and the grain interior next to the TJs are shown in Figs.2 (c & d). Obviously high P peaks can been seen on the spectra collected from the TJ but not in those from grain interior indicating the TJ segregation of P. This is more obvious from the linescan results shown in Figs. 2(e&f). The P concentrations are of 2.7 at% and 4.8 at% at TJ-I and TJ-II, respectively.

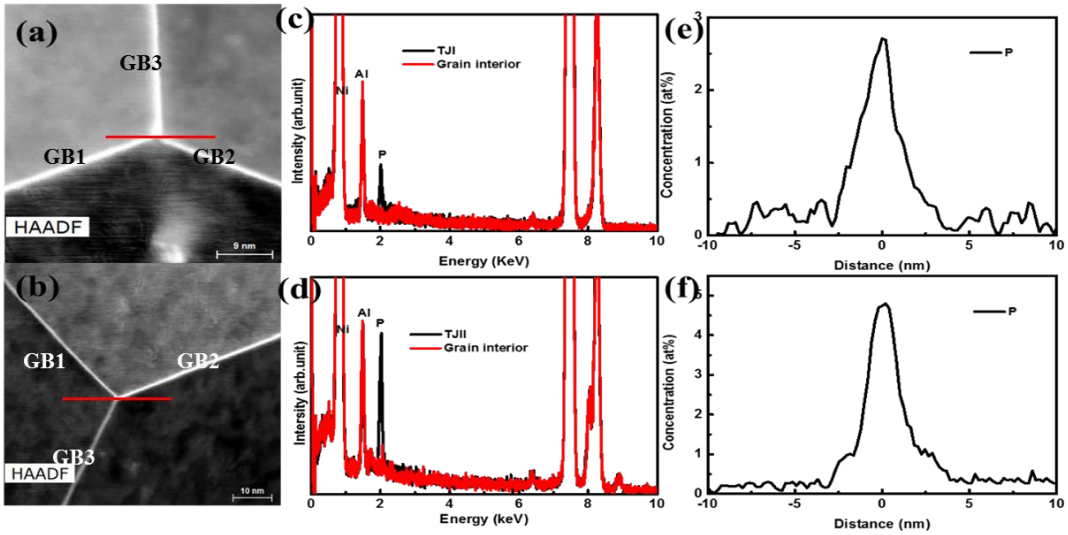

Fig.2 HAADF image of TJ-I (a) and TJ-II (b), and the corresponding spectrum collected from the TJ-I (c) and that from TJ-II (d) together with those from the corresponding grain interiors. The P concentration profiles obtained from the linescan across TJ-I and TJ-II as shown by the red lines in (a) and (b) are presented in (e) and (f), respectively.

Fig.3 shows the EDS elemental maps obtained from the two TJs. GB and TJ segregation of P is obvious. Since the sample was heat-treated at 700 ºC and then water quenched, the

segregation observed can be regarded as non-equilibrium segregation developed during the cooling process. P has been regarded to be substitutional [25, 26] and can diffuse to the grain boundary by forming vacancy-P complexes. The driving force is the concentration gradient of the solute-vacancy complexes between the grain interior and the GB or TJ [27]. Equilibrium segregation during annealing at 700°C can be neglected as the diffusion coefficient of the complexes is several orders of magnitude higher than that of P [7]. This can also be verified by the width of the segregation area measured. Equilibrium segregation width is typically only several atomic layers [28], while the non-equilibrium segregation can be several nanometres wide [29], consistent with the line scan results currently obtained.

Table. 1 Misorientation angles associated with individual GBs and the P concentration measured from each GB, TJ and the adjacent grain interior.

TJ	GB	Misorientation angle (°)	Misorientation axis	GB concentration (at%)	TJ concentration (at%)	Matrix concentration (at%)
TJ-I	GB1	40.8	0.75, 0.53, -0.96	4.0±0.4	2.7±0.3	0.1±0.03
	GB2	42.0	0.88, 0.30, 0.99	3.9±0.4		
	GB3	53.2	0.30, 1.41, 1.04	1.8±0.2		
TJ-II	GB1	43.9	1.33, 0.14, 0.05	4.1±0.4	4.8±0.4	0.1±0.03
	GB2	32.7	-0.05, 0.13, 1.08	3.2±0.3		
	GB3	55.3	-0.59, 1.21, 0.96	1.6±0.2		

As shown in Table 1, the P concentrations at different GBs are different in that GB3 has obviously lower value than GB1 and GB2, in both cases. This is shown more clearly in Fig.4 which presents the spectra collected from the TJs, constituent GBs and adjacent grain interior. The P concentration at GBs varies from 1.6 at.% to 4.1 at.%. This is probably due to the fact that GB free volume acts as the segregation sites for solute atoms, which varies with GB

characters. For instance, calculation has indicated that the free volume varies with the misorientation angles and rotation axes [27].

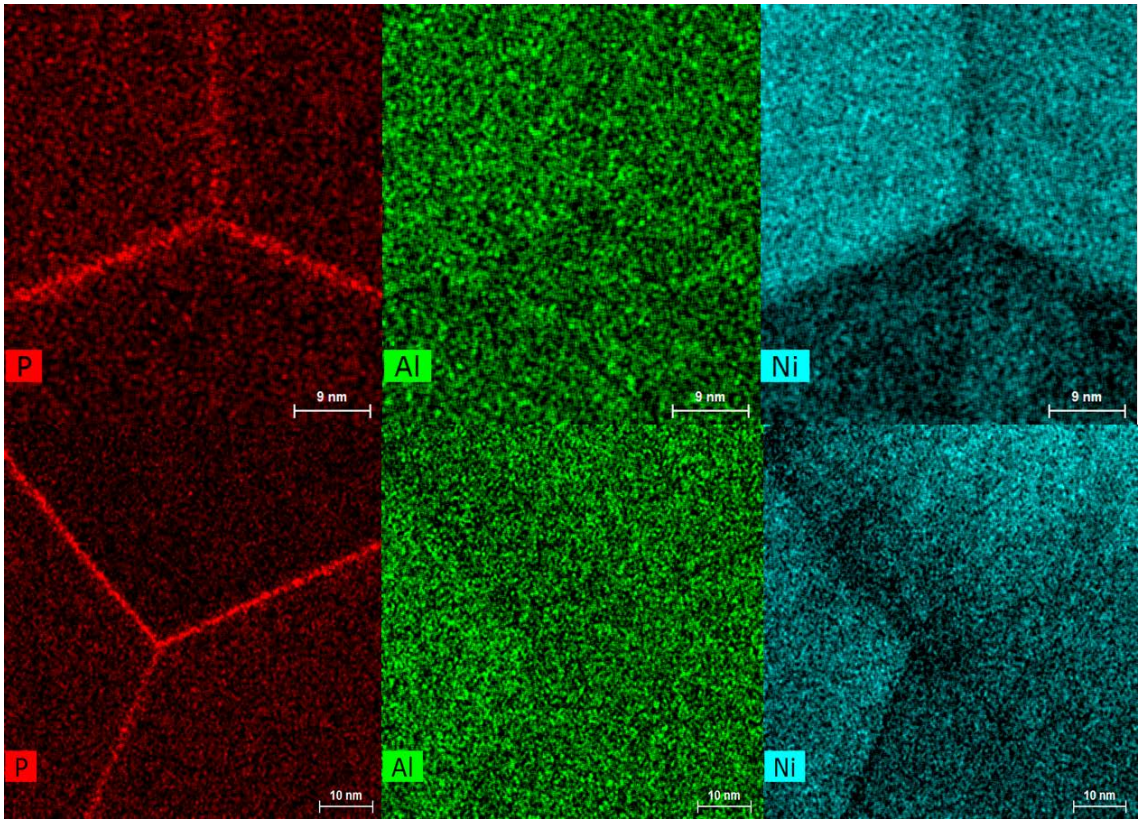

Fig. 3 EDS elemental maps obtained from TJ-I (upper) and TJ-II (lower)

Fig. 4 also shows that the P concentration at TJ-I is higher than that at GB3 but lower than that at GB1 and GB2, while the P concentration at TJ-II is higher than all the constituent GBs, consistent with the results shown in fig.2.

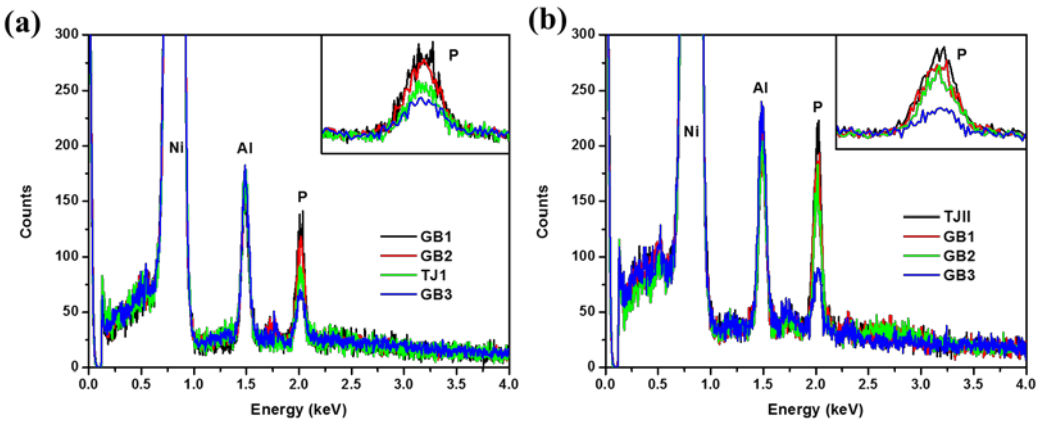

Fig. 4. Comparison of the spectra collected from TJs and constituent GBs shown in fig.2. TJ-I (a) and TJ-2 (b).

In the above measurements, the P concentration on GBs was measured from positions located at least a few hundred of nanometres away from the TJs. The P concentrations along the GBs towards TJ-I were also measured and the results are shown in Fig. 5. While the concentration of P at TJ-I is about 2.7 at%, the concentration of P increased to about 3.9 at% over a distance of about 100 nm from TJ-I along GB2. The concentration of P decreased from 2.7 at% at TJ-I to about 1.8 at% over a distance of about 40 nm along GB3. The P concentration profile along GB1 is characterized with a sharp increase to about 4.0 at% within 5 nm from TJ-I.

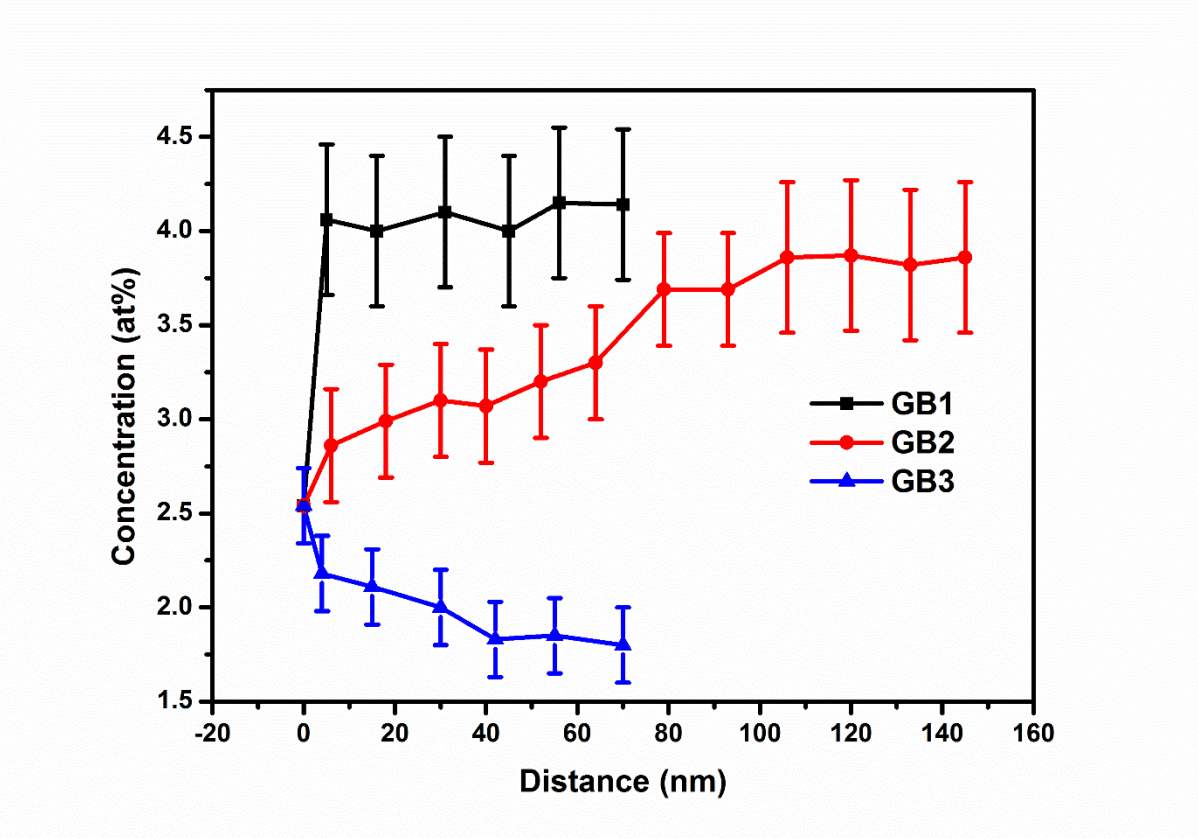

Fig. 5. P concentration profile measured versus the distance from TJ-I along different GBs.

4. Discussion

To the authors' best knowledge, Yin et al [18] reported the first experimental measurement of TJ chemical composition, performed using EDS on a nano-crystalline Cu sample. While their experiment has clearly shown the segregation of Bi to the GB and TJ, no experimental details about the alignment of the GBs and the TJ with the electron beam were given. As mentioned earlier the alignment of a TJ with the electron beam in a nano-crystalline sample would be practically very difficult. Based on a purposely prepared tricrystal foil, Sorbello et al [19] observed the segregation of impurity elements (P and Sn) to the TJ after tilting one of the three GBs to be edge on. More recently, 3D atom probe studies [20-22] have reported the segregation of Bi to the TJs in Ni and C segregation to TJ in steel. Molecular dynamics and Monte Carlo simulation indicated that Mg segregated to TJ in Al and resulted in the formation of nuclei of an ordered phase [30]. Due to the existence of free volume at the TJ, it can serve as the vacancy sinks, just like GB and surface [31]. In the present work, it is likely that the fast cooling during the water quenching from 700 °C led to the vacancy annihilation at TJ and hence the concentration gradient between the grain interior and TJ. It is plausible that the subsequent directional diffusion of the solute-vacancy complex to the TJ thus led to the observed TJ segregation. As suggested in [18], the different TJ concentrations measured can be attributed to the structural differences between the TJs which are dependent on parameters such as the misorientation angles, rotation axes and the constituent grain boundary planes. A quantitative relationship is currently not available and also out of the scope of the current paper, due to the complexity of the TJ structure. The number of degree of freedom needed to describe a TJ and the constituent grain boundaries suggest that misorientation is, but not the sole parameter that one should consider in defining the structure and therefore understanding the chemical segregation at a TJ.

It is generally agreed that a TJ have a larger free volume and therefore a faster diffusion path than the constituent GBs. For instance, the TJ diffusion coefficient of Ni in Cu [10-12], Zn in

Al [32] and Ge in Si [13] was 2-3 orders of magnitude higher than the corresponding GB diffusion coefficients. Molecular dynamics simulation [14] has also confirmed that TJ segregation would be expected due to the large free volume. This is consistent with the experimental results of Bi in Cu where the Bi concentration at TJ was higher than those at both a special GB and random large angle GBs [18]. Monte Carlo simulation result also indicated that Pd is segregated to the TJ more than to special GBs [33]. Along this line, one would expect that the P concentration at TJs should be always higher than that at GBs. However, this contradicts with the current results which show that the P concentration at TJ can be lower than that at the constituent grain boundaries (cf. 2.7 at% at TJ-1 versus 4.0 at% at GB1 and 3.9 at% at GB2). This suggests that the free volume is not the only factor that determines the TJ segregation level. Although the electron probe size is small (0.73 nm), the electron beam spreading within the specimen may lead to the underestimate of the segregation level. The fact that the higher P concentration at TJ-2 than that at all three constituent GBs implies that the segregation of P measurement at the TJ observed cannot be caused by electron beam spreading.

Using Monte Carlo simulation, the segregation of Y in Mg to TJ composed of 2 twin boundaries and 1 random high angle GB was investigated [23]. It was found that Y concentration at TJ is composition dependent and can be lower than random the high angle GB and even the twin boundaries though the average free volume of TJ was always higher than other GBs. A comparison of the segregation and non-segregation site at TJ indicated that some of the atomic Voronoi polyhedrons cannot serve as the segregation site due to a large anisotropic factor. In addition to the volume and anisotropic factor of the Voronoi polyhedron, the shortest interatomic distance and coordination number were regarded as the secondary factors affecting the Y segregation. The simulation results suggested that higher

free volume, smaller anisotropic factor, larger nearest atomic distance and higher coordination number enhance the segregation level [23].

Nonetheless the possibility that the free volume at TJs is lower than that at GBs cannot be excluded. For instance, it has been shown that TJs energy can be comparable or even lower than that of GBs [34, 35]. TJ diffusion coefficient is normally 2-3 orders higher than, but sometimes can also be comparable with, GB diffusion coefficient [36]. Therefore it is plausible that the free volume at TJs can be comparable or even lower than that at the adjacent GBs.

Another possible reason that TJ concentration is not necessarily higher than GBs can be explained by the binding energy and the activation energy of vacancy diffusion. As discussed in [27], vacancy diffusion to a GB results in a gradient of the complex and the enrichment of solutes at GB. So GB diffusion of vacancy plays a key role in determining the segregation level [31]. Using molecular statics modelling along with the nudged elastic band method, the binding energy and the activation energy of vacancy diffusion at several TJs in Al, Cu and Ni were calculated [31]. Due to its large binding energy of up to 1.2 eV, the activation energy of vacancy diffusion in Ni was found to be larger than that in Al and Cu, within the range from 2.26 eV to 2.57 eV. This can be higher than the activation energy of vacancy diffusion along GBs. For example, the activation energy of vacancy diffusion determined using molecular statics based on embedded-atom-method potentials was below 1.8 eV along Σ5 (210) boundaries in Ni [37], which is consistent with the calculation for Σ5 (1.5 eV), Σ11 (1.8 eV) and Σ37 (1.7 eV) GBs [38]. Therefore, the higher activation energy of vacancy diffusion contributes to a slower mobility of the vacancy along TJ and eventually lower the TJ segregation level compared with that at GBs. Therefore the relative segregation level at TJ with regards to that at constituent GBs has contribution from both the structural parameters

such as the free volume, anisotropic factor, atomic distance, coordination number and also atomic diffusion characteristics including the binding energy and activation energy.

As shown in Fig. 4, P concentration on GBs varies with the distance from the TJ. Similar observations have been reported where Bi concentration along GB varies within a distance of 5 nm to 80 nm from a TJ in Cu [14]. Two possible reasons have been proposed regarding the interplay between a TJ and its constituent GBs [18]. If the sample is in equilibrium, the concentration gradient can be attributed to the decaying strain field of the TJ on the constituent GBs [39] which may alter the GB structure, especially the size and/or the geometry of the free volume available for the segregation. If the sample is in non-equilibrium status such as in the case of the current study, the concentration gradient may result from the diffusion of solute atom from TJ to the constituent GBs or in reverse direction, depending on the structural characteristics and atomistic diffusion characteristics.

5. Conclusions

The current work has been demonstrated that a modern STEM EDS system with multi-detectors can effectively be used to detect elemental segregation to GBs and TJs. Non-equilibrium P segregation to TJs has been confirmed in a Ni-base alloy. The P concentration at TJs can be lower or higher than the constituent GBs. The P concentration gradient exists within a distance ranging from a few nanometres to 100 nm from the TJs along the constituent GBs. It is believed that the TJ segregation information could be important for a better understanding of the structure and property evolution of materials such as the grain growth kinetics, the development of functional nano-crystalline materials or in more general term the GB engineering.

Acknowledgements

JT is grateful for a Li Siguang PhD scholarship jointly awarded by the China Scholarship Council and the University of Birmingham.

[1] M. Všianská, M. Šob, The effect of segregated sp-impurities on grain-boundary and surface structure, magnetism and embrittlement in nickel, Prog. Mater. Sci., 56 (2011) 817-840. https://doi.org/10.1016/j.pmatsci.2011.01.008.

[2] J.T. Guo, L.Z. Zhou, The effect of phosphorus, sulphur and silicon on segregation, solidification and mechanical properties in cast Alloy 718, Superalloy 1996, 1996, pp. 451-455.

[3] M. Wang, J. Du, Q. Deng, Z. Tian, J. Zhu, The effect of phosphorus on the microstructure and mechanical properties of ATI 718Plus alloy, Mater. Sci. Eng. A, 626 (2015) 382-389. https://doi.org/10.1016/j.msea.2014.12.094.

[4] W.R. Sun, S.R. Guo, J.H. Lee, N.K. Park, Y.S. Yoo, S.J. Choe, Z.Q. Hu, Effects of phosphorus on the delta-Ni_3Nb phase precipitation and the stress rupture properties in alloy 718, Mater. Sci. Eng. A, 247 (1998) 173-179. https://doi.org/10.1016/S0921-5093(97)00753-3.

[5] W.R. Sun, S.R. Guo, J.T. Guo, B.Y. Tong, Y.S. Yang, X.F. Sun, H.R. Guan, Z.Q. Hu, The common strengthening effect of phosphorus, sulfur, and silicon in lower contents and a problem of a net superalloy, Superalloys 2000, 2000, pp. 467-476.

[6] C.L. Briant, Grain boundary segregation in the Ni-base alloy 182, Metall. Trans. A, 19 (1988) 137-143. https://doi.org/10.1007/BF02669822.

[7] K. Wang, H. Si, C. Yang, T.-d. Xu, Nonequilibrium grain boundary segregation of phosphorus in Ni-Cr-Fe superalloy, J. Iron steel Res., Int., 18 (2011) 61-67. https://doi.org/10.1016/S1006-706X(11)60012-5.

[8] B. Färber, E. Cadel, A. Menand, G. Schmitz, R. Kirchheim, Phosphorus segregation in nanocrystalline Ni–3.6 at.% P alloy investigated with the tomographic atom probe (TAP), Acta Mater., 48 (2000) 789-796. https://doi.org/10.1016/S1359-6454(99)00397-3.

[9] A.H. King, Triple lines in materials science and engineering, Scripta Mater., 62 (2010) 889-893. https://doi.org/10.1016/j.scriptamat.2010.02.020

[10] M.R. Chellali, Z. Balogh, H. Bouchikhaoui, R. Schlesiger, P. Stender, L. Zheng, G. Schmitz, Triple junction transport and the impact of grain boundary width in nanocrystalline Cu, Nano Lett., 12 (2012) 3448-3454. https://doi.org/10.1021/nl300751q

[11] M. Wegner, J. Leuthold, M. Peterlechner, X. Song, S.V. Divinski, G. Wilde, Grain boundary and triple junction diffusion in nanocrystalline copper, J. Appl. Phys., 116 (2014) 093514. https://doi.org/10.1063/1.4893960.

[12] M. Reda Chellali, Z. Balogh, G. Schmitz, Nano-analysis of grain boundary and triple junction transport in nanocrystalline Ni/Cu, Ultramicroscopy, 132 (2013) 164-170. https://doi.org/10.1016/j.ultramic.2012.12.002.

[13] A. Portavoce, L. Chow, J. Bernardini, Triple-junction contribution to diffusion in nanocrystalline Si, Appl. Phys. Lett., 96 (2010) 214102. https://doi.org/10.1063/1.3435476.

[14] T. Frolov, Y. Mishin, Molecular dynamics modeling of self-diffusion along a triple junction, Phys. Rev. B, 79 (2009) 174110. https://doi.org/10.1103/PhysRevB.79.174110.

[15] F. Lefevre-Schlick, Y. Brechet, H.S. Zurob, G. Purdy, D. Embury, On the activation of recrystallization nucleation sites in Cu and Fe, Mater. Sci. Eng. A, 502 (2009) 70-78. https://doi.org/10.1016/j.msea.2008.10.015.

[16] D. Mattissen, D.A. Molodov, L.S. Shvindlerman, G. Gottstein, Drag effect of triple junctions on grain boundary and grain growth kinetics in aluminium, Acta Mater., 53 (2005) 2049–2057. https://doi.org/10.1016/j.actamat.2005.01.016.

[17] D.G. Morris, D.R. Harries, Wedge crack nucleation in Type 316 stainless steel, J. Mater. Sci., 12 (1977) 1587-1597. https://doi.org/10.1007/BF00542809.

[18] K.M. Yin, A.H. King, T.E. Hsieh, F.R. Chen, J.J. Kai, L. Chang, Segregation of bismuth to triple junctions in copper, Microsc. Microanal., 3 (1997) 417-422. https://doi.org/10.1017/S1431927697970318.

[19] F. Sorbello, G.M. Hughes, P. Lejček, P.J. Heard, P.E.J. Flewitt, Preparation of location-specific thin foils from Fe–3% Si bi- and tri-crystals for examination in a FEG-STEM, Ultramicroscopy, 109 (2009) 147-153. https://doi.org/10.1016/j.ultramic.2008.08.011

[20] M. Herbig, D. Raabe, Y.J. Li, P. Choi, S. Zaefferer, S. Goto, Atomic-scale quantification of grain boundary segregation in nanocrystalline material, Phys. Rev. Lett., 112 (2014) 126103. https://doi.org/10.1103/PhysRevLett.112.126103

[21] L. Zheng, M.R. Chellali, R. Schlesiger, Y. Meng, D. Baither, G. Schmitz, Non-equilibrium grain-boundary segregation of Bi in binary Ni(Bi) alloy, Scripta Mater., 68 (2013) 825-828. https://doi.org/10.1016/j.scriptamat.2013.02.002.

[22] M.R. Chellali, L. Zheng, R. Schlesiger, B. Bakhti, A. Hamou, J. Janovec, G. Schmitz, Grain boundary segregation in binary nickel–bismuth alloy, Acta Mater., 103 (2016) 754-760. https://doi.org/10.1016/j.actamat.2015.11.003.

[23] N. Miyazawa, S. Suzuki, M. Mabuchi, Y. Chino, An atomistic study of Y segregation at a $\{10\bar{1}1\}$–$\{10\bar{1}2\}$ double twin in Mg, AIP Adv., 7 (2017) 035308. https://doi.org/10.1063/1.4978534.

[24] P. Schlossmacher, D.O. Klenov, B. Freitag, H.S. von Harrach, Enhanced detection sensitivity with a new windowless xeds system for aem based on silicon drift detector technology, Microsc. Today, 18 (2010) 14-20. https://doi.org/10.1017/S1551929510000404.

[25] D. Connétable, É. Andrieu, D. Monceau, First-principles nickel database: Energetics of impurities and defects, Comput. Mater. Sci., 101 (2015) 77-87. https://doi.org/10.1016/j.commatsci.2015.01.017.

[26] S. Zhang, X. Xin, L. Yu, A. Zhang, W. Sun, X. Sun, Effect of phosphorus on the grain boundary cohesion and γ′ precipitation in IN706 alloy, Metall. Mater. Trans. A, 47 (2016) 4092-4103. https://doi.org/10.1007/s11661-016-3495-6.

[27] T.D. Xu, B.Y. Cheng, Kinetics of non-equilibrium grain-boundary segregation, Prog. Mater. Sci., 49 (2004) 109-208. https://doi.org/10.1007/BF01160590.

[28] D. Terentyev, X. He, E. Zhurkin, A. Bakaev, Segregation of Cr at tilt grain boundaries in Fe–Cr alloys: A Metropolis Monte Carlo study, J. Nucl. Mater., 408 (2011) 161-170. https://doi.org/10.1016/j.jnucmat.2010.11.024.

[29] E.P. Simonen, S.M. Bruemmer, Cr-vacancy elastic and chemical interactions in irradiated stainless steels, MRS Proc., 540 (2011) 501. https://doi.org/10.1557/PROC-540-501.

[30] I.N. Karkin, L.E. Karkina, A.R. Kuznetsov, M.V. Petrik, Y.N. Gornostyrev, P.A. Korzhavyi, Segregation of Mg to generic tilt grain boundaries in Al: Monte Carlo modeling, Mater. Phys. Mech., 24 (2015) 201-210.

[31] I. Adlakha, K.N. Solanki, Structural stability and energetics of grain boundary triple junctions in face centered cubic materials, Sci. Rep., 5 (2015) 8692. https://doi.org/10.1038/srep08692.

[32] B. Bokstein, V. Ivanov, O. Oreshina, A. Peteline, S. Peteline, Direct experimental observation of accelerated Zn diffusion along triple junctions in Al, Mater. Sci. Eng., A, 302 (2001) 151-153. https://doi.org/10.1016/S0921-5093(00)01367-8.

[33] Y. Purohit, L. Sun, D.L. Irving, R.O. Scattergood, D.W. Brenner, Computational study of the impurity induced reduction of grain boundary energies in nano- and bi-crystalline Al–

Pb alloys, Mater. Sci. Eng., A, 527 (2010) 1769-1775. https://doi.org/10.1016/j.msea.2009.11.034.

[34] G. M. Poletaev, D. V. Dmitrienko, V. V. Dyabdenkov, V. R. Mikryukov, M. D. Starostenkov, Triple junctions of inclined and mixed grain boundaries in nickel, Steel Transl., 43 (2013) 180–183. https://doi.org/10.3103/S096709121304013X.

[35] S. G. Srinivasan, J. W. Cahn, H. Jonsson, G. Kalonji, Excess energy of grain-boundary trijunctions: an atomistic simulation study, Acta Mater., 47 (1999) 2821–2829. https://doi.org/10.1016/S1359-6454(99)00120-2.

[36] B.S. Bokstein, A.O. Rodin, B.B. Straumal, Self-diffusion parameters of grain boundaries and triple junctions in nanocrystalline materials, Defect Diffus. Forum, 309-310 (2011) 45-50. https://doi.org/10.4028/www.scientific.net/DDF.309-310.45.

[37] R.T. Murzaev, A.A. Nazarov, Activation energy for vacancy migration in [001] tilt boundaries in nickel, Phys. Met. Metallogr., 101 (2006) 86-92. https://doi.org/10.1134/S0031918X06010121.

[38] A. Arjhangmehr, S.A.H. Feghhi, A. Esfandiyarpour, F. Hatami, An energetic and kinetic investigation of the role of different atomic grain boundaries in healing radiation damage in nickel, J. Mater. Sci., 51 (2016) 1017-1031. https://doi.org/10.1007/s10853-015-9432-z.

[39] S. Shekhar, A.H. King, Strain fields and energies of grain boundary triple junctions, Acta Mater., 56 (2008) 5728-5736. https://doi.org/10.1016/j.actamat.2008.07.053.